Frozen capillary waves on glass surfaces: an AFM study

T. Sarlat, A. Lelarge, E. Søndergård, and D. Vandembroucq[a]

Laboratoire "Surface du Verre et Interfaces", Unité Mixte CNRS/Saint-Gobain, 39 quai Lucien Lefranc,
93303 Aubervilliers Cedex, France

Abstract. Using atomic force microscopy on silica and float glass surfaces, we give evidence that the roughness of melted glass surfaces can be quantitatively accounted for by frozen capillary waves. In this framework the height spatial correlations are shown to obey a logarithmic scaling law; the identification of this behaviour allows to estimate the ratio $kT_F/\pi\gamma$ where k is the Boltzmann constant, γ the interface tension and T_F the temperature corresponding to the "freezing" of the capillary waves. Variations of interface tension and (to a lesser extent) temperatures of annealing treatments are shown to be directly measurable from a statistical analysis of the roughness spectrum of the glass surfaces.

PACS. 68.35.Ct Interface structure and roughness – 61.43.Fs Glasses – 68.03.Cd Surface tension and related phenomena – 68.37.Ps Atomic force microscopy (AFM)

1 Introduction

Glass is becoming a widespread substrate in high-tech developments like flat displays [1], thin foiled X-ray telescope mirrors [2] and lithography masks [3]. In all of these applications, controlling the glass surface roughness is a critical issue to enhance performance. Glass manufactures spend considerable effort in optimizing their forming process. The introduction in the late fifties of the float process to produce flat glass represented a revolution in the glass industry: the glass sheets obtained in this way are almost perfectly flat so that the expensive polishing step revealed to be unnecessary for most applications. The process somehow mimics and extends the traditional method of fire polishing. The latter consists of first heating the surface to a temperature high enough to obtain local melting and then quenching the resulting smooth surface. Laser polishing [4] can be seen as another modern extension of the same strategy. In the float process, the molten glass flows from the furnace on a liquid tin bath. The (liquid) glass thus spreads out on the tin surface to form a ribbon. The progressive cooling imposed along the tin bath allows the two glass surfaces (tin/glass and glass/atmosphere) to freeze without external mechanical contact. Note that similar comments could be made about other glass forming processes like fiber drawing.

The residual roughness of these "fire polished" surfaces is extremely low, typically below the nanometer range when measured over a micrometric scale and has been attributed to the freezing of the capillary waves of the liquid interface in the glass transition temperature range [5].

This particular phenomenon has recently been studied on glycerol [6,7] and supercooled polymers [8] by X-ray reflectivity. Though the surface roughness induced by capillary waves is long range correlated, the X-ray reflectivity of a liquid surface was shown to depend mainly on the total interface width $\sigma \propto kT/\gamma$ [9], where k is the Boltzmann constant, T the temperature and γ the interface tension. When varying temperature in the glass transition regime, a clear saturation of the interface roughness was obtained below a threshold temperature [6–8]. A satisfactory quantitative agreement with a capillary waves description is obtained in the case of polymers; for glycerol, however, a density driven layering effect was suspected, only a qualitative agreement could be obtained.

In this paper, we present a detailed quantitative atomic force microscopic (AFM) study of the roughness spectrum of melted glass surfaces, namely silica surfaces obtained after various annealing treatments and bare industrial float glass surfaces. AFM has previously been used to study the roughness of glass surfaces [10]; but only recently, a few reports [11,12] have been given of a qualitative agreement between the values of the roughness measured on glass surfaces and the simple estimates obtained from a description of the surface in terms of frozen capillary waves $\sigma \approx kT_G/\gamma$. Here again, σ is the standard deviation of the height fluctuations along the surface (RMS roughness), γ the surface tension of the glass and the glass transition temperature T_G is used as an estimate of the freezing temperature of capillary waves. Focusing on two different glass surfaces (silica and float glass) we show here that the height correlations along the surface give a direct and quantitative access to the frozen capillary wave spatial spectrum. The use of these two different materials

[a] e-mail: `damien.vdb@saint-gobain.com`

allows us study two different aspects of the phenomenon. Performing heat treatments on silica at different temperatures in the glass transition range we can study the effect of thermal history on the glass surface roughness. Performing measurements on the two faces (namely "tin" and "atmosphere") of a float glass, we can test the effect of the two different interface tensions due to the asymmetry of the float process.

The paper is organised as follows. We first recall some results on capillary waves at a liquid interface and we give quantitative expressions expected for the height correlations in this framework. Then we detail the experimental protocol and we finally present the AFM measurement results obtained respectively on silica and float glass. Finally we discuss their interpretation in terms of frozen capillary waves.

2 Capillary waves

Assuming a constant value of the surface tension γ, the excess of energy $E(h)$ due to the height fluctuations $h(x_1, x_2)$ of a liquid interface can be estimated to:

$$E(h) = \gamma \int \left(\sqrt{1 + |\nabla h^2|} - 1 \right) dx_1 dx_2, \qquad (1)$$

$$\simeq \frac{\gamma}{2} \int |\nabla h|^2 dx_1 dx_2, \qquad (2)$$

where x_1, x_2 are the horizontal coordinates and γ the interface tension. Using a Boltzman distribution, we easily obtain the expressions of the RMS roughness σ and of the spatial correlation function $G(r)$ and of the height variogram $H(r)$:

$$\sigma^2 = \langle h^2(\overrightarrow{x}) \rangle_{\overrightarrow{x}} = \frac{kT}{2\pi\gamma} \ln \left(\frac{\lambda_M}{\lambda_m} \right) \qquad (3)$$

$$G(r) = \langle h(\overrightarrow{x} + \overrightarrow{r}) h(\overrightarrow{x}) \rangle_{\overrightarrow{x}} = \frac{kT}{2\pi\gamma} \ln \left(\frac{\lambda_M}{r} \right) \qquad (4)$$

$$H(r) = \langle |h(\overrightarrow{x} + \overrightarrow{r}) - h(\overrightarrow{x})|^2 \rangle_{\overrightarrow{x}} = \frac{kT}{\pi\gamma} \ln \left(\frac{r}{\lambda_m} \right) \qquad (5)$$

where $\overrightarrow{x} = x_1 \overrightarrow{e_1} + x_2 \overrightarrow{e}_1$ and $r = |\overrightarrow{r}|$. As the expressions are logarithmically divergent, an upper (λ_M) and a lower (λ_m) spatial cut-off must be introduced. Gravity effects are neglected in the above description and the upper cut-off is given by the capillary length $\ell_c = \sqrt{\gamma/\rho g}$ where ρ is the glass density and g is the gravity constant. For silica ($\gamma \simeq 0.3 \ \mathrm{J \, m^{-2}}$, $\rho \simeq 2.2 \ \mathrm{kg \, m^{-3}}$) this length is approximatively equal to 4 mm. The lower cut-off is estimated to a molecular length ℓ_0. For silica and silicate glasses in general the structural unit is the SiO_4 tetrahedron, and we can take $\ell_0 \simeq 0.5$ nm. Using equation (3), the typical roughness of a silica surface in the glass transition region ($T_G \simeq 1450$ K) due to capillary waves can thus be estimated to $\sigma \approx 0.4$ nm. In a first approximation we consider that the interface height fluctuations freeze at

this glass transition temperature T_G so that equations (3–5) can be used to describe the roughness of the glass surfaces at room temperature simply replacing T by T_G. A detailed treatment of the freezing of capillary waves based on the visco-elasticity theory can be found in [5].

Molecular and capillary lengths thus define the ultimate physical bounds of the expected logarithmic scaling. However, in the framework of roughness measurement, the cut-off lengths are imposed by the limited bandwidth of the experimental set-up. In the context of atomic force microscopy the scan size, usually in the micromemeter range, defines the upper cut-off λ_M and the nanometric tip radius (or the sampling length) define the lower cut-off λ_m.

3 Experimental method

We detail here the sample preparation (annealing treatment for silica and cleaning procedure) and on the roughness data extraction from the raw AFM data.

3.1 Sample preparation

3.1.1 Float glass

Float glass is a standard industrial product with approximate composition: SiO_2 72%, Na_2O 14%, CaO 9%, MgO 4%. Note that due to the asymmetry of the float process some traces of Sn are present in the vicinity of the "tin" surface. 1 cm^2 samples were cut from a 3 mm thick glass sheet. No additional treatment but cleaning (described below) was performed on these surfaces.

3.1.2 Silica

The silica samples are commercial silica wafers (vitreosil, EQ512), 2 mm-thick, two side polished. Square samples of 1 cm × 1 cm were prepared. Prior to the annealing treatment, the sample preparation was as follows: the sample is supported on a finely grained silicon carbide plate, Saint-Gobain Ceramics, and covered by a platinum lid, the entire system is placed on a fire-brick. Fire-brick, platinum lid, silicon carbide plate and samples are cleaned with the same protocol: (i) one ultra-sonic cleaning of fifteen minutes in a millipore water/detergent (aquanox) 10% mixture; (ii) two ultra-sonic rinsing of fifteen minutes in millipore water; (iii) drying with dry nitrogen. After this cleaning, all pieces are placed in a furnace at 60 °C to dry the porous fire-brick.

3.1.3 Annealing treatments on silica

All silica samples were first submitted to a high temperature treatment: 1770 K during 30 min. This step is performed well above the $T_G \simeq 1450$ K to ensure full relaxation of surface defects due to the polishing step. The sample is then immediately taken out from the furnace;

Table 1. Thermal history of samples.

Sample	1500	1350	1200	1100
A	30 min			
B	30 min	60 min		
C	30 min		120 min	
D	30 min			68 h

the platinum cap is only removed after 10 min in order to avoid dust in-layering on the molten surface.

Beyond this surface relaxation step, the silica samples have undergone different thermal treatments to test the dependence of surface roughness on thermal history. We followed annealing protocols proposed by Le Parc et al. [13] who studied the effect of thermal history on the Raman spectrum of silica. The thermal treatments are listed in Table 1. Annealing times have been calculated to allow silica relaxation. After annealing, each sample is removed from the furnace in the same condition as described above.

Note that the long annealing time applied to sample D has caused a slight nucleation of a crystalline phase of silica under the surface. This is not expected to affect further interpretations as the crystals were subsurface.

3.1.4 Post-annealing cleaning

In order to eliminate contaminations due to storage and transport, samples were cleaned before AFM measurements. We checked that the surface was not altered by successive cleaning operations. The previous cleaning protocol was used. A last step is added: a 45 min UV/O_3 cleaning to remove nanometric dust and also to obtain a hydrophilic surface improving surface imaging. Despite these precautions some dust was found on the surfaces. However, AFM scans show large dust free parts (typically 15 μm $\times$ 15 μm).

3.2 Quantitative use of AFM for surface morphology

The surface morphology of all samples have been characterized by AFM height measurement in tapping mode (TM-AFM), using a Nanoscope III A from Digital Instruments with Al coated tip (BudgetSensors — model BS-Tap 300 Al). The Al coating thickness is 30 nm, the resonant frequency is 300 kHz and the stiffness constant is 40 Nm^{-1}. The tip radius is lower than 10 nm. The images have been recorded at a scan frequency between 0.8 and 1Hz for a resolution of 512×512 pixels.

As our study is focused on the analysis of extremely smooth surfaces, special attention has to be paid to the data treatment. The roughness induced by capillary waves lies indeed in the sub-nanometer range and corresponds to the ultimate thermodynamic fluctuations of the interface. At this low roughness level, limitations of AFM can be observed in the bare data.
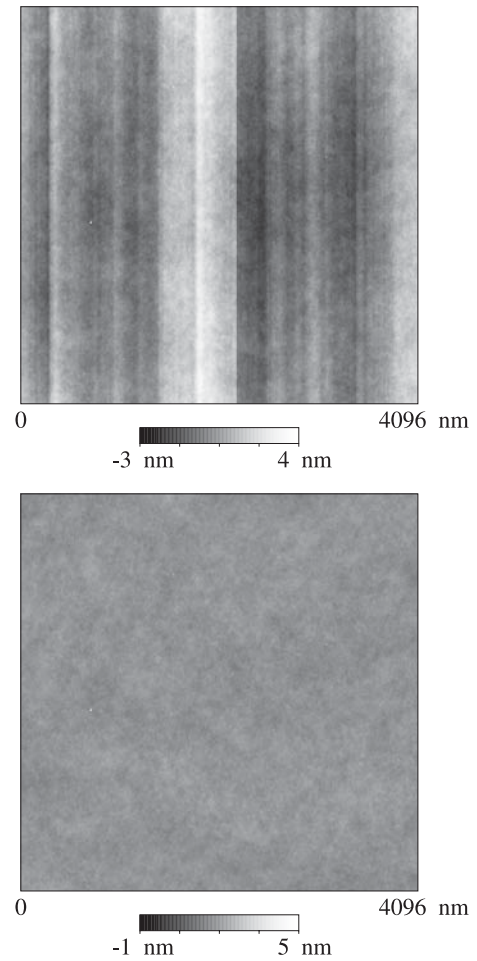
Fig. 1. An image of an annealed silica surface (A) acquired in the open air. (a) correction by the best fitted paraboloid ($\sigma_{rms} = 0.43$ nm) to compensate the systematic curvature effect due to the spherical motion of the piezo-electric stage, note the residual bands due to a drift error of the tip; (b) correction by the best set of parabolas ($\sigma_{rms} = 0.25$ nm).

The sample is moved by a XYZ-piezo-electric stage and long profiles exhibit a slight spherical character. This systematic curvature in the height data can be eliminated by subtracting the best paraboloid to the surface. Figure 1a shows the result of this first operation. A remaining strong band pattern is observed; this results from a drift error of re-positioning of the piezo-electric stage. Strictly speaking AFM measurements thus have to regarded as a set of profiles more than an image and bare data must be corrected line by line. Figure 1b shows a representative AFM image obtained after subtraction of the best set of parabolas (in a least mean square sense) to the set of profiles. The statistical analysis is thus performed on these profiles.

4 Results

4.1 Silica

A set of AFM roughness measurements on the samples A, B, D has been made in order to determine the
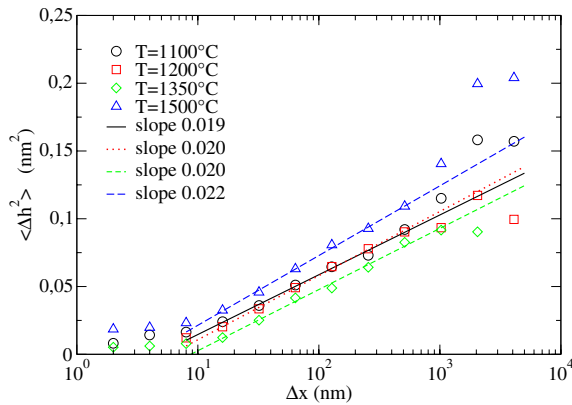
Fig. 2. Height variogram obtained from AFM measurements on silica surfaces after various annealing treatments in the glass transition regime (symbols). The lines correspond to the predicted logarithmic behaviour induced by the presence of frozen capillary waves (fit performed in the interval [16 nm–500 nm]).

Fig. 3. Height variogram obtained from AFM measurements on the two faces of a float glass, respectively in contact with liquid tin and with atmosphere (symbols). The fitted lines correspond to the logarithmic behaviour predicted by the presence of frozen capillary waves (fit performed in the interval [8 nm–2000 nm]).

scaling behaviour of the roughness from the nanometer range up to the micrometer range. The typical experiment is the following: a first image is acquired over $8\ \mu m \times 8\ \mu m$, then a hierarchy of images of decreasing size ($4\ \mu m$, $2\ \mu m$... down to 512 or 128 nm depending on the sample) is taken within this first image. We performed the measurements of 2 such series down to 128 nm for sample A; 2 series down to 512 nm for sample B and 3 series down to 512 nm for sample D. On sample C we measured 14 images of $2\ \mu m \times 2\ \mu m$ and 7 sets of 2 imbricated images of respective size $8\ \mu m \times 8\ \mu m$ and $2\ \mu m \times 2\ \mu m$.

The statistical treatment consisted in computing the height variogram on each individual image and to average these data for the different images of a series. We thus obtain in Figure 2, the evolution of the average quadratic height difference $H(r) = \langle |h(x+r) - h(x)|^2 \rangle_x$ between points on the surface separated by a distance r. In the semi-log scale used in Figure 2, we obtain a linear behaviour over more than 2 decades from a few nanometers up to a few micrometers. We thus obtain a very good agreement with the predicted capillary wave scaling proposed in equation (3). The values of the slopes obtained by a simple linear fit in the scaling region are reported in Table 2. A physical discussion on these extracted parameters and the quantitative agreement with the theory is given in Section 5.

4.2 Float glass

Using the same procedure as above, 6 sets of images of decreasing size from $8\ \mu m \times 8\ \mu m$ down to 500 nm × 500 nm were performed on the atmosphere and tin faces of the float glass samples. The atmosphere faces were more affected by residual dust pollution and only 3 of them could be quantitatively analysed. The height variograms are displayed in semi-log scale in Figure 3. Again we observe a logarithmic behaviour over more than two decades. The values of the slopes obtained by a simple linear fit in the
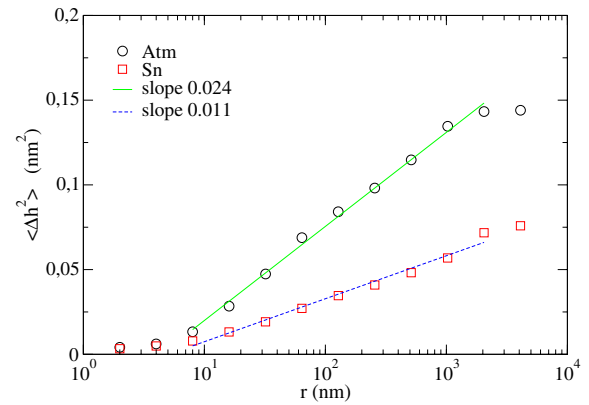
Table 2. Estimation of the capillary wave slope parameter obtained by fitting the evolution of the mean square: $H(r) = ar + b$ and comparison with reference values $a_{th} = kT_F/\pi\gamma$ obtained from the annealing temperatures and estimates of the interface tensions.

Sample	T_F(K)	γ (J/m^2)	a_{th} (nm^2)	a (nm^2)
silica A	1773	0.3	0.026	0.022 ± 0.003
silica B	1623	0.3	0.024	0.020 ± 0.003
silica C	1473	0.3	0.022	0.020 ± 0.003
silica D	1373	0.3	0.020	0.019 ± 0.003
float atm.	873	0.35	0.011	0.024 ± 0.004
float tin	873	0.5	0.008	0.011 ± 0.002

scaling region are reported in Table 2. The tin face appears to be much smoother than the atmosphere face, which is consistent with the smaller interface tension expected for the glass atmosphere interface compared with the tin/glass interface.

4.3 Statistical averaging, uncertainty

To evaluate the accuracy of our results, we investigated the dispersion of the roughness measurements. This was done on the silica sample C. As a first test, 14 images of size $2\ \mu m$ were recorded within a primary zone of size $8\ \mu m$. The mean value of the height variances obtained on these images was $\sigma^2 = 0.029$ nm^2 and the standard deviation 0.005 nm^2, that is to say 15% of the mean value. As a second test, we performed 7 sets of 2 imbricated images of respective sizes $8\ \mu m$ and $2\ \mu m$ measured at different places over the surface. For the $8\ \mu m$ scans, we obtain a mean value of 0.053 nm^2 and a root mean square of 0.007 nm^2 that is to say 15% of the mean value. For the $2\ \mu m$ we found a mean value of 0.030 nm^2 and a root mean square of 12% of the mean value. We can conclude that we have roughly a dispersion of 15% of the mean value. This

gives us an estimate of the uncertainty on our roughness measurements and on the numerical parameters used to fit the logarithmic behaviour predicted by equation (5).

5 Discussion

As shown in Figures 2 and 3 the height variograms show a clear logarithmic behaviour from the nanometer range up to the micrometric range. Table 2 shows a summary of the parameters characterising the frozen capillary wave regime. As references, we indicated the values $kT_F/\pi\gamma$ corresponding to the annealing temperatures used for silica and the temperature of the soda-lime glass at the end of the float tank; we used generally accepted estimates of the interface tensions silica/air, glass/air and tin/glass at high temperature [15–17].

Several comments can be made upon these results. First, within experimental errors we obtain a clear logarithmic scaling of the spatial correlation with physical parameters consistent with the scenario of capillary waves freezing.

In this naive scenario we assume that the surface freezes at a well-defined temperature T_F. Some more complex phenomena may characterise the freezing step, in particular one can think of a dependence of the freezing temperature on the spatial frequency dependence of the capillary waves. However such glassy behaviours, leading to departures from the simple logarithmic scaling could not be identified within experimental errors.

The logarithmic behaviour could be observed over 2 to 3 decades from the nanometer range to the micrometer range. Our data do not show any clear upper cut-off. Our AFM set-up being limited to a maximum scan length of 17 μm, larger scales were not explored. Note however that the pollution of the surfaces by dust or impurities makes it more and more difficult to analyse the data beyond 10 μm. As discussed above, the lower cut-off of the logarithmic range is supposed to correspond to an atomic length scale. In our case, this cut-off has an instrumental origin and amounts to a few nanometers, which correponds to the AFM tip resolution. Note again that the logarithmic scaling induces a divergence for both small and large scales. Variations of the lower cut-off value due to a change of rounding of the AFM tip thus may induce a vertical shift of the roughness data (see Eq. (5)).

In this framework of frozen capillary waves, the slope measured in the semi-log plot is directly related to the ratio T_F/γ where T_F is the freezing temperature and γ the interface tension.

In the case of silica we observe first a very good agreement between experimental slopes and references values. We observe a very low growing tendency of this slope with the annealing temperature. This may thus correspond to a slight increase of the effective freezing temperature but this tendency is certainly not clear enough to give any firm conclusion. The typical slope obtained around 0.20 nm^2 are very close to the value 0.22 nm^2 corresponding to the glass transition temperature of silica $T_G = 1450$ K and

an interface tension $\gamma = 0.3$ J m^{-2}. Let us note in addition that, because of thermal inertia, it is not surprising that for the annealing processes at high temperature the effective freezing temperature (the experimental slope) be lower than the annealing temperature (the reference slope).

In the case of float glass we observe a striking contrast between the two faces. The tin face is noticeably smoother than the atmosphere face as can be expected from the contrast of interface tensions. Focusing on the quantitative aspect, we note that the experimental slopes are quite higher than the reference values, particularly in the case of the atmosphere face. This may obviously be due to an underestimation of the freezing temperature and/or an overestimation of the interface tensions. Let us insist on the latter point, the experimental measurement of interface tensions at high temperature (sessile drop methods and further evolutions) remains delicate and large variations of the measured values can be found in literature [15]. The interface tension can indeed be very dependent on the atmosphere and on the composition.

6 Conclusion

Performing AFM roughness measurements on annealed silica surfaces and on float glass surfaces we could confirm that the roughness of "fire polished" glasses can be quantitatively described by frozen capillary waves in the micrometric range. In particular we could identify a clear dependence of the roughness spectrum on the interface tension and we obtain indications of a slight dependence upon the freezing temperature. At length scales below the capillary length, the industrial float process thus allows to produce flat glass surfaces characterised by the lowest thermodynamically possible roughness; the only way of reducing these fluctuations would consist of increasing the interface tension or of decreasing the "freezing" temperature of capillary waves. In addition, we could show that the description of glass surfaces by capillary waves gives access to the ratio freezing temperature on interface tension T_F/γ and can thus be considered as a complementary indirect way of measuring the two quantities.

References

1. Some Technical aspects of glass substrates for TFT LCD applications, A. Shiou Glass Techol. **44** 148 2003
2. Y. Soong, K.W. Chan, P.J. Serlemitsos, Proc. SPIE, **4496**, 54–61 (2001)
3. U. Behringer, H. Seitz, F. Sobel, M. Renno, T. Leutbecher, N. Olschewski, T. Reichart, R. Walter, H. Becker, U. Buttgereit, G. Hess, K. Knapp, C. Wies, R. Lebert, Proc. SPIE **5835**, 244 (2005)

4. F. Vega, N. Lupón, J. Armengol Cebrian, F. Laguarta, Opt. Eng. **37**, 272 (1998)

5. J. Jäckle, K. Kawasaki, J. Phys.: Cond. Mat. **7**, 4351 (1995)

6. T. Seydel, M. Tolan, B.M. Ocko, O.H. Seeck, R. Weber, E. DiMasi, W. Press, Phys. Rev. B **65**, 184207 (2002)

7. A. Madsen, T. Seydel, M. Sprung, C. Gutt, M. Tolan, G. Gršubel, Phys. Rev. Lett. **92**, 096104 (2004)

8. M. Sprung, T. Seydel, C. Gutt, R. Weber, E. DiMasi, A. Madsen, M. Tolan, Phys. Rev. B **70**, 051809 (2004)

9. B.M. Ocko, X.Z. Wu, E.B. Sirota, S.K. Sinha, M. Deutsch, Phys. Rev. Lett. **72**, 242 (1994)

10. D. Abriou, Y. Levillain, H. Arribart, F. Creuzet, *International symposium on glass problems* (Istanbul, 1996)

11. P.K. Gupta, D. Innis, C.R. Kurkjian, Q. Zhong, J. Non-Cryst. Solids **262**, 200 (2000)

12. P.J. Roberts, F. Couny, H. Sabert, B.J. Mangan, D.P. Williams, L. Farr, M.W. Mason, T.A. Birks, J.C. Knight, P.St.J. Russel, Opt. Express **13**, 236 (2005)

13. R. Le Parc, B. Champagnon, Ph. Guenot, S. Dubois, J. Non-Cryst. Solids, **293**–**295**, 367 (2001)

14. J.V. Sengers, J.M.J. van Leuwen, Phys. Rev. A **39**, 6346 (1989)

15. H. Scholze, *Le Verre* (Institut du Verre, Paris, 1980)

16. J. Barton, C. Guillemet, *Le verre, science et technologie* (EDP Sciences, Paris, 2005)

17. V.I. Nizhenko, Yu.I. Smirnov, Powder Metall. **42**, 171 (2003)